

## $\delta_{25}$ Crack opening displacement parameter in cohesive zone models: experiments and simulations in asphalt concrete

S. H. SONG<sup>1</sup>, M. P. WAGONER<sup>2</sup>, G. H. PAULINO<sup>3</sup> and W. G. BUTTLAR<sup>3</sup>

<sup>1</sup>Department of Transportation, 1801 30th Street, Sacramento, CA 91816, USA, <sup>2</sup>ATK Tactical Propulsion and Controls, Allegany Ballistics Laboratory, 210 State Route 956, Rocket Center, WV 26726, USA, <sup>3</sup>Department of Civil and Environmental Engineering, University of Illinois at Urbana-Champaign, Newmark Laboratory, 205 North Mathews Avenue, Urbana, IL 61801, USA

Received in final form 14 August 2008

**ABSTRACT** Recent work with fracture characterization of asphalt concrete has shown that a cohesive zone model (CZM) provides insight into the fracture process of the materials. However, a current approach to estimate fracture energy, i.e., in terms of area of force versus crack mouth opening displacement (CMOD), for asphalt concrete overpredicts its magnitude. Therefore, the  $\delta_{25}$  parameter, which was inspired by the  $\delta_5$  concept of Schwalbe and co-workers, is proposed as an operational definition of a crack tip opening displacement (CTOD). The  $\delta_{25}$  measurement is incorporated into an experimental study of validation of its usefulness with asphalt concrete, and is utilized to estimate fracture energy. The work presented herein validates the  $\delta_{25}$  parameter for asphalt concrete, describes the experimental techniques for utilizing the  $\delta_{25}$  parameter, and presents three-dimensional (3D) CZM simulations with a specially tailored cohesive relation. The integration of the  $\delta_{25}$  parameter and new cohesive model has provided further insight into the fracture process of asphalt concrete with relatively good agreement between experimental results and numerical simulations.

**Keywords**  $\delta_{25}$ ; asphalt concrete; disk-shaped compact tension (DC(T)); three-dimensional cohesive zone model.

### INTRODUCTION

Asphalt concrete is used as a surfacing material for pavement structures throughout the world with vast sums of money being invested into the maintenance of these pavement structures. Although there are many distresses, or causes of deterioration, associated with asphalt concrete, a major concern is the fracture of the asphalt concrete, which decreases the serviceability of the structure. Until recently, empirical relationships have been utilized to develop design approaches that reduce the likelihood of the pavement structure fracturing.<sup>1</sup> However, these empirical approaches are limited to specific pavement structures, since extrapolating the design approaches to different pavement designs (pavement thickness, materials, environmental effects, etc.) may not result in good performing pavements. The movement in recent years in the asphalt concrete pavement community has been to incorporate fundamental mechanics into the pavement designs that would allow for the prediction of pavement perfor-

mance over a wide range of design variables.<sup>2</sup> Specifically, fracture mechanics is being applied to characterize the mechanisms that initiate and propagate a crack through asphalt concrete by using experimental techniques and computational mechanics.<sup>3–8</sup>

Asphalt concrete has been shown to exhibit quasi-brittle fracture where the softening of the material can be attributed to the microstructure where the aggregates have the ability to interlock and slide while the asphalt mastic displays cohesion and viscoelastic properties. Currently, researchers are implementing the cohesive zone model (CZM) approach to describe the fracture process of asphalt concrete. One of the material properties that are required for the CZMs is the fracture energy, or the energy required to fully separate the material. Work conducted by Wagoner et al.<sup>5</sup> suggests that the fracture energy of asphalt concrete can be obtained by using a disk-shaped compact tension specimen, DC(T), in which the fracture energy is obtained by using the CMOD of the specimen. This is utilized since the CMOD is a measurement required to perform the experiment. The main disadvantage of using the CMOD for obtaining fracture energy

Correspondence: G. H. Paulino. E-mail: paulino@uiuc.edu

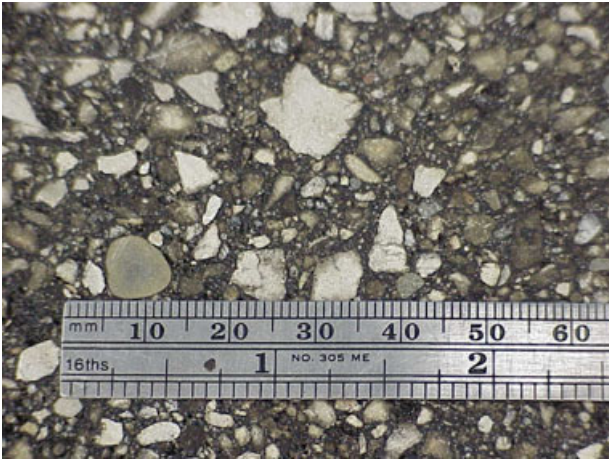


Fig. 1 Typical asphalt concrete microstructure.

is that the CMOD is a quantity which includes contributions from both material separation and bulk material deformation. Thus, the fracture energy is usually over predicted when using the CMOD.<sup>9</sup>

In this work, we introduce a new displacement measurement,  $\delta_{25}$ , to provide a local quantity of CTOD. The papers of Schwalbe *et al.* provided the framework for the  $\delta_{25}$  measurement with their work on the  $\delta_5$  quantity.<sup>10–12</sup> The  $\delta_5$  measurement was developed and applied to fine-grained materials with great success. The challenge with applying the  $\delta$ -measurement to asphalt concrete is the coarse microstructure that has aggregates as large as 25 mm (see Fig. 1 for typical asphalt concrete microstructure). For this current study, the maximum aggregate size in the asphalt concrete mixture is 9.5 mm, therefore, the measurement at the notch tip is obtained over a 25 mm gauge length to ensure that the influence of the aggregates become negligible from the measurements. As a general rule for heterogeneous mixtures, such as asphalt concrete, the gauge length should be approximately 3 times the maximum aggregate size.<sup>13</sup> The fracture energy obtained from the  $\delta_{25}$  parameter may provide better estimation for asphalt concrete mixtures, since the compliance associated with the global response is either reduced or eliminated. The work herein will go on to describe the usefulness of the  $\delta_{25}$  parameter.

## MATERIALS AND METHODS

The development of the  $\delta_{25}$  measurement is conducted using a disk-shaped compact tension, DC(T), specimen. The DC(T) test has been successfully developed for determining the fracture energy of asphalt concrete<sup>5</sup>. In addition to the typical measurements, the test set-up for the  $\delta_{25}$  measurements required two extra clip gauges to be attached to the specimen at the notch tip. Gauges are

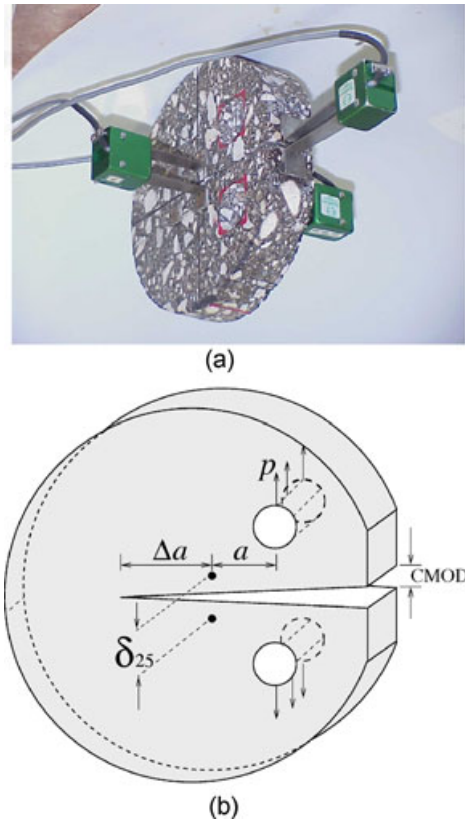


Fig. 2 Fracture parameter  $\delta_{25}$  in DC(T) test specimen: (a) experimental setting; (b) schematic drawing. Notice that  $a$  indicates the original crack length and  $\Delta a$  denotes a distance between the original crack tip and the current crack tip.

attached to the specimen at a gauge length of 25 mm on both sides of the specimen (see Fig. 2). The data presented herein is obtained at a single test temperature of  $-20^\circ\text{C}$  and a constant CMOD rate of  $1\text{ mm min}^{-1}$ . This CMOD rate was chosen to have a similar rate to the AASHTO T322 strength test.<sup>14</sup> The material used for the test is obtained from a pavement located in northeast Iowa. Along with the fracture energy, the tensile strength of the material is required as an input into the CZM and is determined by using AASHTO T322-03 standard test method for determining the creep compliance and strength of hot mix asphalt (HMA) using the indirect tensile test device.<sup>14</sup>

## POWER-LAW COHESIVE ZONE MODEL

The shape of a CZM in quasi-brittle materials is as important as the basic cohesive parameters, i.e., fracture energy and material strength. The effective displacement,  $\delta$ , and the effective traction,  $t$ , for three-dimensional (3D) analysis become

$$\delta = \sqrt{\delta_n^2 + \delta_s^2} = \sqrt{\delta_n^2 + \delta_{s1}^2 + \delta_{s2}^2} \quad (1)$$

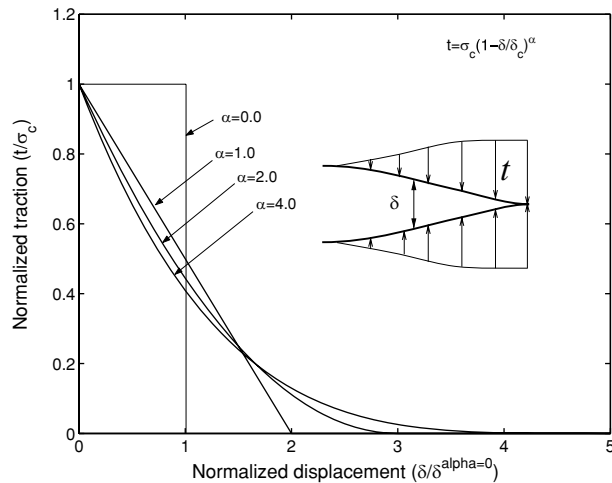


**Fig. 3** Cohesive model in terms of displacement jumps and corresponding tractions for different  $\alpha$  values. Notice that, for simplicity, the elasticity part of the cohesive zone model is not plotted.

$$t = \sqrt{t_n^2 + t_s^2} = \sqrt{t_n^2 + t_{s1}^2 + t_{s2}^2} \quad (2)$$

in which  $\delta_{s1}$  and  $\delta_{s2}$  denote components of shear sliding displacement ( $\delta_s$ ), and  $t_{s1}$  and  $t_{s2}$  are components of shear traction ( $t_s$ ). The power-law CZM<sup>15</sup> can be expressed as

$$t = \sigma_c(1 - \delta/\delta_c)^\alpha, \quad (3)$$

in which  $t$  is traction,  $\sigma_c$  is material strength,  $\delta_c$  is critical displacement where a complete separation, i.e., zero traction, occurs, and  $\alpha$  is an internal variable governing the shape of the softening curves. The  $\delta_c$  is obtained by equating the area under the curve to the fracture energy which is given as

$$G = \int_0^{\delta_c} t d\delta = \int_0^{\delta_c} \sigma_c(1 - \delta/\delta_c)^\alpha d\delta = \frac{1}{1 + \alpha} \sigma_c \delta_c. \quad (4)$$

Figure 3 illustrates various shapes of the power-law cohesive zone models. The ordinate is normalized traction and the abscissa is displacement which is normalized with respect to critical displacement with  $\alpha = 0$ . When  $\alpha$  is equal to zero, it is a rectangular shape. As  $\alpha$  increases, the shape of the softening curves changes from the linear curve to nonlinearly decaying curves. For simplicity, the elasticity part of the model is not addressed nor plotted in the figure. Detailed theoretical and numerical aspects can be found in previous work by the authors.<sup>7,15</sup>

## EXPERIMENTS AND VALIDATION

The fracture energy is determined using the DC(T) specimen at  $-20^\circ\text{C}$  and a CMOD rate of  $1 \text{ mm min}^{-1}$ . Note that identically sized specimens are used to minimize size effect on fracture energy, since the primary emphasis of

**Table 1** Fracture energy of the two replicates at  $-20^\circ\text{C}$

Replicate	Fracture energy		
	CMOD	$\delta_{25}$ (face 1)	$\delta_{25}$ (face 2)
1	181	116	117
2	200	129	118
Average	191	120	

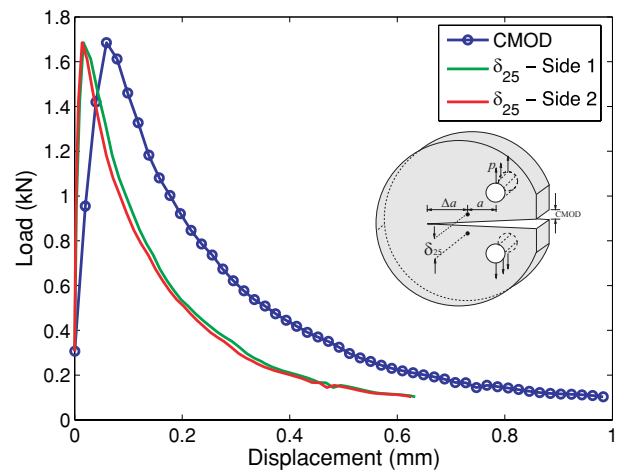


**Fig. 4** Load versus displacement of CMOD and  $\delta_{25}$  (experimental results).

this paper is to demonstrate the new  $\delta_{25}$  measurement in conjunction with cohesive zone fracture modeling. The size effect phenomenon associated with the fracture of concrete<sup>16–17</sup> and asphalt<sup>18–19</sup> has been well documented in other studies. The energy is calculated using both the CMOD and  $\delta_{25}$  measurements. Two replicates are tested and the results are shown in Table 1. ASTM D7313-07b states that a minimum of three replicate specimens should be used to determine the fracture energy of asphalt concrete.<sup>5</sup> For the particular testing performed in this study, however, only two replicates per test condition were available due to field sampling. Despite this shortcoming, the experimental data reported herein were found to be adequate for illustrating the usefulness of the  $\delta_{25}$  parameter. The average fracture energy calculated using the CMOD is  $191 \text{ J m}^{-2}$ , while the fracture energy calculated from the  $\delta_{25}$  measurement is  $120 \text{ J m}^{-2}$ . The difference between the CMOD and  $\delta_{25}$  measurements can be seen in Fig. 4. The initial slope of the load-CMOD curve up to the peak is greater for the  $\delta_{25}$  measurements. Therefore, the  $\delta_{25}$  measurement is not measuring the extraneous compliance that is associated with the CMOD measurement.

Another important experimental finding from the  $\delta_{25}$  measurement is the difference in the shape and rate of the displacements. The CMOD is utilized as the test control and had a constant opening rate of  $1 \text{ mm min}^{-1}$ . The  $\delta_{25}$

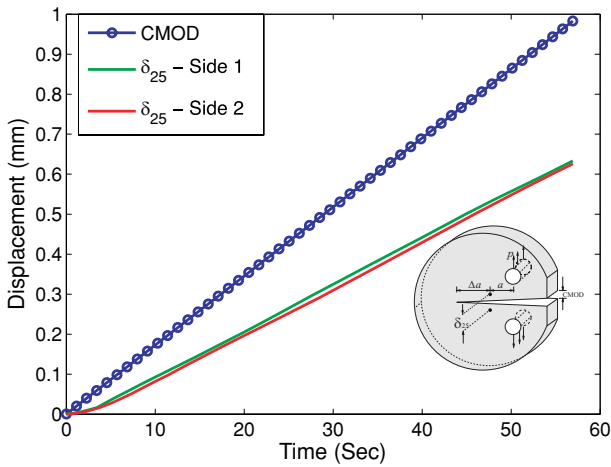


Fig. 5 Displacement versus time for CMOD and  $\delta_{25}$  (experimental results).

measurements does not show a constant opening rate. As shown in Fig. 5, the  $\delta_{25}$  measurement showed a nonlinear response up to a point, then a linear response. Typical results have shown that the inflection point where the  $\delta_{25}$  measurement rate becomes constant is close to the peak load. This might suggest that the macro-crack had initiated at the notch tip and started to propagate, where the  $\delta_{25}$  measurement would be at constant rate. Further investigation is needed on this topic.

**COMPUTATIONAL RESULTS**

Figure 6(a) illustrates a DC(T) specimen which is 143 mm high, 139 mm long and 35 mm thick. The length of the mechanical notch,  $a$ , is 26.5 mm, leading to  $a/w=0.25$ . Displacement control inducing a constant CMOD rate of  $1.0 \text{ mm min}^{-1}$  is adopted. Fig. 6(b) shows three dimensional mesh discretizations for the whole geometry. The DC(T) test specimen is constructed using 28094 8-node brick elements for the bulk material and 840 8-node elements for cohesive materials. The cohesive elements are inserted along the middle of specimen to enable the simulation of pure mode-I crack propagation. Symmetry condition along the thickness direction is employed to reduce the computational cost. A constant Poisson’s ratio is used:  $\nu = 0.35$ . The fracture energy obtained at  $-20^\circ\text{C}$  and  $1 \text{ mm min}^{-1}$  loading rate is  $190 \text{ J m}^{-2}$  in the context of CMOD, and the material strength measured at  $-20^\circ\text{C}$  is 2.90 MPa. Prony series parameters (see Table 2) evaluated from experiment of IDT test are adopted for viscoelastic analysis of bulk materials.

Figure 7 (a) shows comparison of present numerical results with experimental results. In this simulation, the power-law CZM<sup>20</sup> with  $\alpha = 1$  (see Fig. 3) is employed and fracture energy evaluated in conjunction with the CMOD is adopted. The present numerical results overpredict

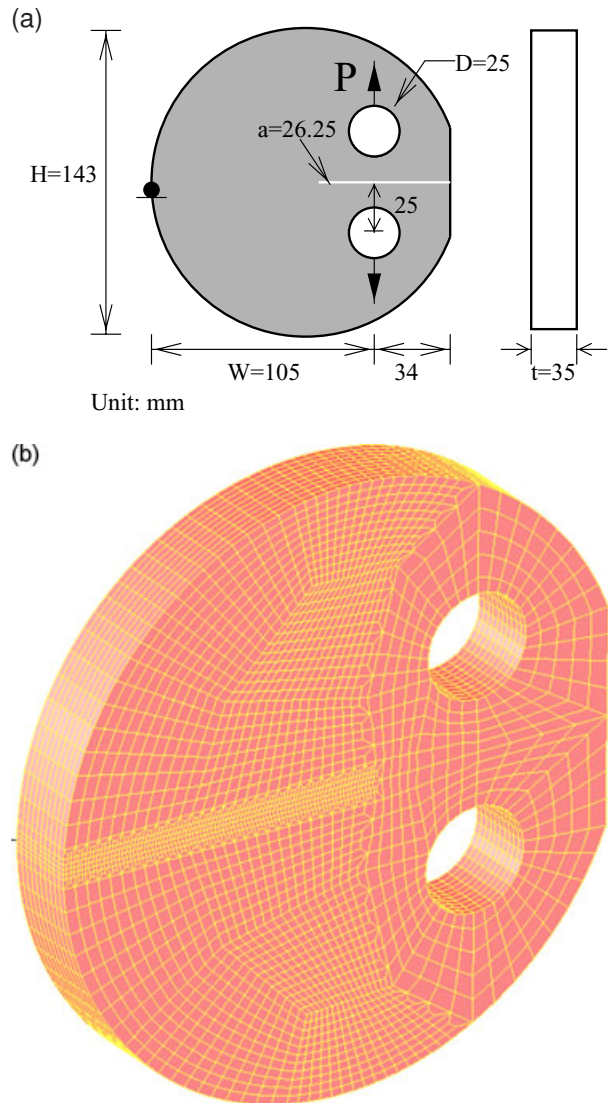
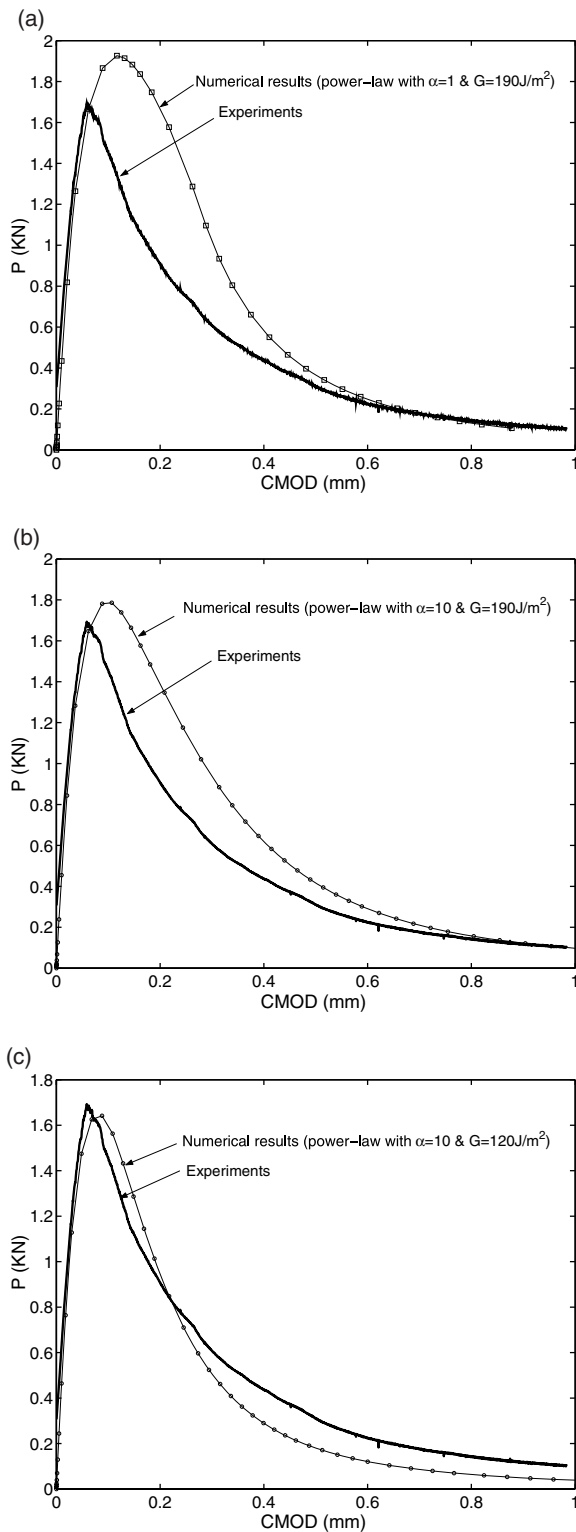


Fig. 6 DC(T) test simulation: (a) geometry and boundary conditions; (b) mesh configuration for the whole geometry.

Table 2 Prony series parameters for the master relaxation modulus using the generalized Maxwell model

<i>i</i>	Relaxation modulus parameters	
	$E_i$ (GPa)	$\tau_i$ (sec)
1	3.54	15
2	3.43	249
3	1.75	4817
4	7.21	57 378
5	11.92	2 605 452

both the peak load and the area under the curve, which concurs with findings reported in previous studies.<sup>18</sup> Furthermore, the discrepancy between numerical and experimental results is very significant around the



**Fig. 7** Comparison of numerical results with experimental results: (a) The power-law model with  $\alpha = 1$  and  $G = 190 \text{ J m}^{-2}$ ; (b) The power-law model with  $\alpha = 10$  and  $G = 190 \text{ J m}^{-2}$ ; and (c) The power-law model with  $\alpha = 10$  and  $G = 120 \text{ J m}^{-2}$ . Notice that the fracture energy computed using CMOD and  $\delta_{25}$  is  $G = 190 \text{ J m}^{-2}$  and  $G = 120 \text{ J m}^{-2}$ , respectively.

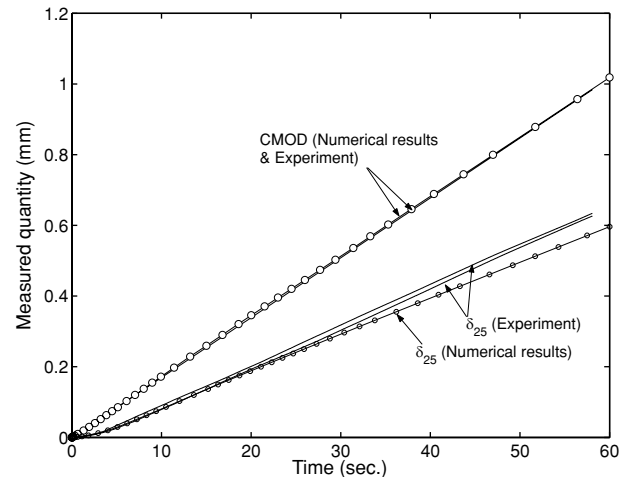


**Fig. 8** Time versus CMOD and  $\delta_{25}$ . Notice that in this simulation, the proposed model is employed and the fracture energy is evaluated in conjunction with the  $\delta_{25}$  parameter.

peak load and becomes small as the crack approaches the boundary. Figure 7(b) compares numerical results, which are obtained using both the power-law with  $\alpha = 10$  and fracture energy associated with CMOD, with experimental results. It is clearly demonstrated that the peak load and the softening trend of the present numerical results are quite similar with those of the experiments. Still, the area under the curve of numerical modeling is bigger than that of the experiments. This indicates that the energy evaluated in conjunction with the CMOD is overestimated. This is intuitive because when the CMOD is employed to compute fracture energy, the energy consumption in the bulk material and along the fracture plane contributes to the evaluation of the fracture energy. Figure 7(c) illustrates both experimental results and numerical results. In the modeling, the power-law with  $\alpha = 10$  is used and the energy  $120 \text{ J m}^{-2}$  evaluated in conjunction with the  $\delta_{25}$  is employed. The  $P$  versus CMOD curve of the present numerical results favorably matches with that of experiments. Especially, up to the CMOD 0.2 mm, both numerical and experimental results have very good agreement.

Figure 8 illustrates time versus displacement, i.e., the CMOD and the  $\delta_{25}$ , of experiments and numerical results. The CMOD of both numerical results and experiments are identical which is expected because it was a prescribed boundary condition in the test (i.e., the test device was operated with closed-loop control, enforcing a linear increase of CMOD with time). For the  $\delta_{25}$ , numerical results match favorably with experimental results. Especially, both the numerical results and experimental results have a very close deflection point. From this simulation, it is inferred that the combination of the two new approaches leads to good agreement between numerical results and experiments without artificial calibration

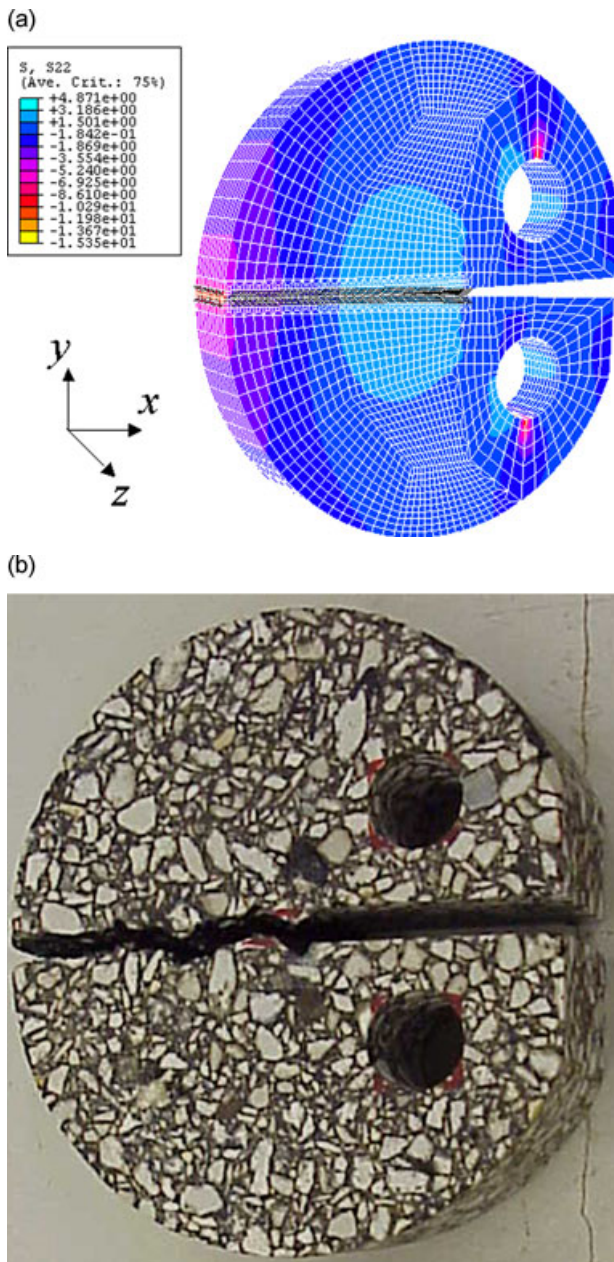


**Fig. 9** Numerical and experimental results: (a)  $\sigma_{yy}$  on the deformed shape when the P reaches the peak point). Magnification factor 50 is used for the deformed shape; (b) actual cracked specimen.

factor(s). Figure 9 (a) illustrates  $\sigma_{yy}$  on the deformed shape when the load P reaches the peak point. To make crack propagation visible, a magnification factor of 50 is employed. Figure 9(b) shows an actual cracked specimen, which demonstrates a mode-I dominant fracture pattern.

## CONCLUSIONS

For convenience, fracture energy measurement in asphalt concrete typically involves the use of a CMOD

measurement for test control and for computation of experimental fracture energy. However, due to the contribution of the bulk and fracture to computation of fracture energy, its evaluation based upon CMOD is overestimated and as a result, calibration procedures in numerical modeling are not avoidable.<sup>6</sup> In this study, the  $\delta_{25}$  parameter is proposed as an operational definition of crack tip opening displacement (CTOD) in asphalt concrete. The use of the  $\delta_{25}$  parameter in evaluating fracture energy leads to more reasonable numerical results due to the fact that the  $\delta_{25}$  is closer to local quantity than the CMOD, which is validated in this study. Furthermore, there is significant improvement in modeling when a nonlinearly decaying softening curve, e.g., the power-law CZM with  $\alpha = 10$ , is employed. The integration of the  $\delta_{25}$  parameter and new cohesive model has provided further insight into the fracture process of asphalt concrete with good agreement between the experimental results and numerical simulations.

## Acknowledgements

We are grateful to the support from the Koch Materials Company (presently SemMaterials, L. P.) and the National Science Foundation (NSF) through the GOALI project CMS 0219566 (Program Manager, P. N. Balaguru). Any opinions expressed herein are those of the writers and do not necessarily reflect the views of the sponsors.

## REFERENCES

- Huang, Y. H. (1993) *Pavement Analysis and Design*. Prentice Hall, New Jersey.
- Guide for Mechanistic-Empirical Design of New and Rehabilitated Pavement Structures. Technical Report, 2004.
- Soares, J. B., Colares de Freitas, F. A. and Allen, D. H. (2003) Crack modeling of asphaltic mixtures considering heterogeneity of the material. *Transportation Research Board*, 82<sup>nd</sup> Annual Meeting, Washington, D.C. (Compendium of Papers CD-ROM).
- Li, X. and Marasteanu, M. (2004) Evaluation of the low temperature fracture resistance of asphalt mixtures using the semi-circular bend test. *J. Assoc. Asphalt Paving Technol.* **73**, 401–426.
- Wagoner, M. P., Buttlar, W. G. and Paulino, G. H. (2005) Disk-shaped compact tension test for asphalt concrete fracture. *Exp. Mech.* **45**, 270–277.
- Song, S. H., Paulino, G. H. and Buttlar, W. G. (2006) A bilinear cohesive zone model tailored for fracture of asphalt concrete considering viscoelastic bulk material. *Eng. Fract. Mech.* **73**, 2829–2848.
- Song, S. H. (2006) Fracture of asphalt concrete: A cohesive zone modeling approach considering viscoelastic effects. PhD thesis. University of Illinois at Urbana-Champaign.
- Wagoner, M. P., Buttlar, G. H., Paulino, W. G. and Blankenship, P. (2006) Laboratory testing suite for

- characterization of asphalt concrete mixtures obtained from field cores. *Proc. Assoc. Asphalt Paving Technol.* **75**, 815–852.
- 9 Shah, S. P., Swartz, S. E. and Ouyang, C. (1995) *Fracture mechanics of concrete: Applications of fracture mechanics to concrete, rock, and other quasi-brittle materials*, John Wiley and Sons, New York.
  - 10 Schwalbe, K.-H. (1995) Introduction of  $\delta_5$  as an operational definition of the CTOD and its practical use. In: *Fracture Mechanics Volume 26: Volume*, ASTM STP 1256, American Society for Testing and Materials, Philadelphia, pp. 763–778.
  - 11 Schwalbe, K.-H., Ainsworth, R. A., Saxena, A. and Yokobori, T. (1999) Recommendations for a modification of ASTM E1457 to include creep-brittle materials. *Eng. Fract. Mech.* **62**, 123–142.
  - 12 Schwalbe, K.-H., Newman, Jr. J. C. and Shannon, Jr. J. L. (2005) Fracture mechanics testing on specimens with low constraint—Standardisation activities within ISO and ASTM. *Eng. Fract. Mech.* **72**, 557–576.
  - 13 Romero, P. and Masad, E. (2001) Relationship between the representative volume element and mechanical properties of asphalt concrete. *ASCE J. Mater. Civil Eng.* **13**, 77–84.
  - 14 AASHTO (2004) *Standard test method for determining the creep compliance and strength of hot mix asphalt (HMA) using the indirect tensile test device*. Standard Specifications for Transportation Materials and Methods of Sampling and Testing, 24th Edition.
  - 15 Song, S. H., Paulino, G. H. and Buttlar, W. G. Three-dimensional power-law cohesive zone model for fracture modeling in asphalt concrete, submitted for publication.
  - 16 Wagoner, M. P. (2007) *Fracture test for bituminous-aggregate mixtures: Laboratory and field investigation*. PhD thesis, University of Illinois at Urbana-Champaign.
  - 17 Wagoner, M. P. and Buttlar, W. G. (2007) Influence of specimen size on fracture energy of asphalt concrete. *Proc. Assoc. Asphalt Paving Technol.* **76**, 391–426.
  - 18 Bazant, Z. P. and Planas, J. (1998) *Fracture and Size Effect in Concrete and other Quasibrittle Materials*. CRC Press, Boca Raton, FL.
  - 19 Park, K. (2005) Concrete fracture mechanics and size effect using a specialized cohesive zone model. Master's thesis, University of Illinois at Urbana-Champaign.
  - 20 Espinosa, H. D. and Zavattieri, P. D. (2003) A grain level model for the study of failure initiation and evolution in polycrystalline brittle materials. Part 1. Theory and numerical implementation. *Mech. Mater.* **35**, 333–364.